Fracture of brittle discs under biaxial loading

A. Börger[1] and P. Supancic[1]

[1] Institute for Structural and Functional Ceramics
University of Leoben
AUSTRIA

ABSTRACT: *In industrial mass production ceramic parts are often disc shaped, especially when producing electroceramics. To be able to assure a constant quality or to trace changes in the production cycle a quick, cheap and meaningful mechanical testing of samples of different production batches has to be performed. Often used approaches for the direct testing of disc shaped specimens are either the Brazilian disc test or different disc flexure tests. A very common disc flexure test is the ring-on-ring test. This test as well as a modification of it, the ring-of-balls on ring-of-balls test, is quite easy to perform and to evaluate but the gained results of these test assemblies are very vulnerable to geometric imperfections of the tested disc and the support rings.*
In this paper a special variant of a disc flexure test will be discussed, the so called ball on three balls test. In this test configuration a disc is supported by three balls and then axially loaded from the opposite side via a fourth ball. Through to the loading on three well defined points this test is quite tolerant to a slight out of flatness of the disc.
Caused by the three support balls the stress state in the disc is not axisymmetric but shows a threefold symmetry making an exact analytical assessment of the stress state in the loaded disc rather difficult. Therefore former estimations of the stress amplitude are quite inaccurate. In this paper a FE analysis of the stress field was performed and different equivalent stress models were investigated and compared with the results of experiments of uniaxial bent bar and biaxial bent disc Al_2O_3 specimens. Furthermore fractography was used to localise the fracture origin on the tested Al_2O_3 discs and bars.

INTRODUCTION

Biaxial strength testing of brittle materials has been used for many years, and there exists a wide variety of test assemblies described in the literature. Typically, there are several advantages claimed for biaxial flexural testing of discs compared with uni-axial testing (in tension or in bending), including ease of test piece preparation, use for thin sheet materials and testing of a large surface area free from edge finishing defects [1]. Furthermore many commercially produced components are biaxially loaded and for them biaxial testing is –compared to uniaxial testing- the more relevant test condition.

A very common specimen geometry for biaxial strength tests is a disc shaped sample. Several biaxial test methods for discs are known and most of them are well described in the literature [2, 3, 4, 5]. In generally they can be classified into two different groups of test assemblies. The first class is a test assembly which leads to a axisymmetric stress field in the specimen, the second one leads to a non- axisymmetric stress field.

To get an axisymmetric stress field the specimen needs a circular line support and is loaded from the opposite side either centrally by a punch or ball or by a smaller circular, concentric line load. The most common axisymmetric test geometry is the ring-on-ring test [2]. This test is easy to perform and to evaluate but also show often a quite significant scatter of the results. Mostly this is caused by the influence of a small out of flatness of the disc which leads to an undefined loading condition [2].

A common non axisymmetric loading condition is given by a set-up of three support balls and a loading centrally from the opposite side of the disc. This leads to a fairly high tolerance to any out of flatness of the disc, since the three considered support points always lead to a stable mechanical condition. On the other hand the resulting stress field in the specimen is more complicated as for instance compared to a bending bar

As in a former paper shown [6] the analytical solutions for the stress field that are offered in the literature [7, 8] are unsatisfactory for the calculation of the maximum tensile stress in the disc as they are based on thin plate theory. Therefore a 3D Finite Element investigation of the stress field in the disc has been performed [6].

For a comparison of the test results of this biaxial strength test with the results of other test methods (e.g. the 4-point bending test, where an uniaxial stress state occurs) two things have to be taken into account. First the effectively loaded volume or surface of the specimens and second for the biaxial stress state an adequate equivalent stress modell.

Experimental set-up

The set up of the ball on three balls test is quite simple and can be seen in figure 1.

The test assembly consists of six parts numbered from 1 to 6. These parts are: the single loading ball (1), the three support balls (2 to 4), the inner piston (5) and the centring device (6). The centring device all centres the loading ball, the sample and the three support balls which allows very accurate and reproducible positioning of these parts relative to each other.

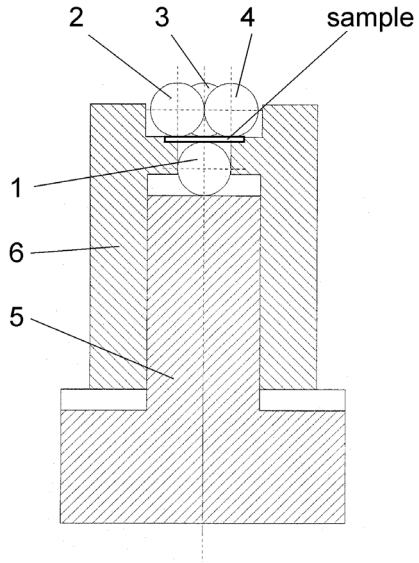

Figure 1: Experimental set-up of the ball on three balls test.

For the experiment the whole test assembly is inserted into a standard universal tester. The three support balls are brought in contact with the punch from tester, the centring device is lowered to allow bending of the disc and the load on the balls is increased until fracture of the disc occurs. The maximum load (i.e. fracture load) is measured and used for evaluation purposes.

Finite Element model of the test rig

As already stated above the test assembly is quite simple and allows a quick strength testing of disc shaped samples. To be able to obtain comparable strength values of the sample the individual fracture loads during the test have to be converted to stress values in the disc. As the test assembly shows a threefold symmetry this conversion is not trivial. Different analytical solutions for the stress distribution and for the maximum tensile stress in the disc are provided in the literature [1, 2, 5, 7, 8] but they differ quite significantly in the calculated stress values. To be able to use this test as a reliable strength test therefore the test assembly was modelled by the Finite Element (FE) method. By taking advantage of the symmetries the model could be reduced to the modelling of a sixth of the test assembly as can be seen in figure 2a.

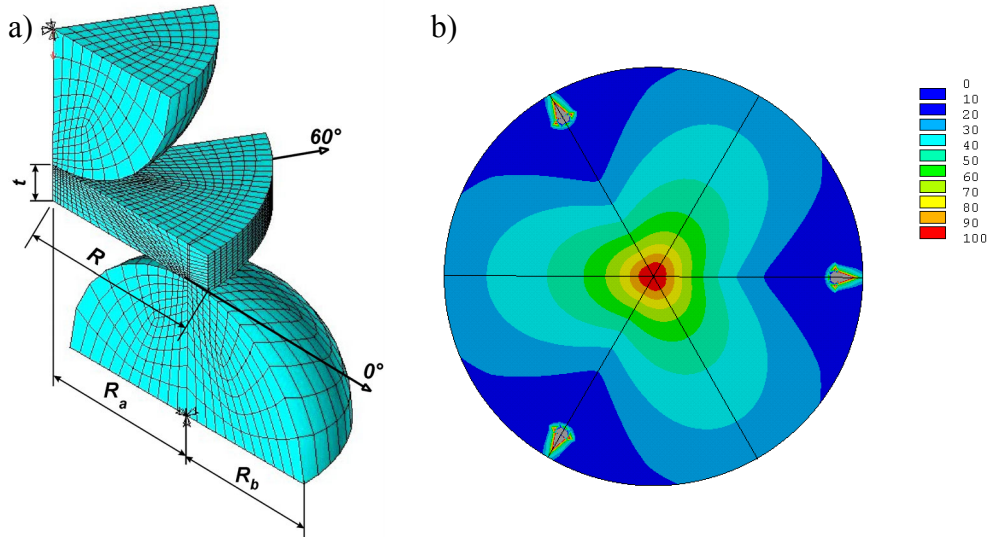

Figure 2 a: Finite Element model of a sixth of the test assembly. The disc has the radius R and the thickness t, the loading and support balls have the radius R_b. The support ball touches the disc in the distance R_a from its centre, the loading ball contacts the disc at its centre.
2 b: Example distribution of the first principle stress on the tensile stress surface of the disc. The stress is scaled from 0 to 100%. The maximum stress is in the centre of the surface where an equibiaxial stress state occurs.

An example of a resulting stress distribution on the tensile stress surface of the disc for a ratio t/R = 0.2 and R_a/R= 0.87 can be seen in figure 2b. The maximum stress is in the centre of the tensile surface of the disc. At this point there exists an equibiaxial stress state. As already mentioned the stress distribution shows a threefold symmetry and the tensile stress decreases rather rapidly with radial distance from the disc centre. The maximum tensile stress can be calculated according to equation (1):

$$\sigma_{\max} = f \cdot \frac{F}{t^2}, \qquad (1)$$

with the maximum load at fracture, F, the disc thickness, t, and a dimensionless factor f. This factor f is a function of the disc geometry (t and R), the support radius R_a and the Poisson's ratio, ν, according to:

$$f\left(\frac{t}{R},\frac{R_a}{R},\nu\right)=c_0+\frac{\left(c_1+c_2\frac{t}{R}+c_3\left(\frac{t}{R}\right)^2+c_4\left(\frac{t}{R}\right)^3\right)}{1+c_5\frac{t}{R}}\left(1+c_6\frac{R_a}{R}\right), \qquad (2)$$

with the fitting constants c_0 to c_6 according to table 1.

TABLE 1: Constants for f depending on ν

	ν = 0.2	ν = 0.25	ν = 0.3
c_0	-12.354	-14.671	-17.346
c_1	15.549	17.988	20.774
c_2	489.2	567.22	622.62
c_3	-78.707	-80.945	-76.879

	ν = 0.2	ν = 0.25	ν = 0.3
c_4	52.216	53.486	50.383
c_5	36.554	36.01	33.736
c_6	0.082	0.0709	0.0613

For ceramic materials the location of the maximum stress it not necessarily also the location of the fracture origin. This is an effect of the distribution of defects which leads to a distribution of strength within the specimen [9, 10]. Therefore two different specimen geometries or two different stress distributions can only be compared if the effective loaded volume (for volume sensitive tests) or the effective loaded surface (for surface sensitive tests) is known [11]. This effective volumes and surfaces can be calculated according to equations (3) and (4) by integrating the normalised stress distribution in the specimen:

$$V_{eff}=\int_V\left(\frac{\sigma_e(x,y,z)}{\sigma^*}\right)^m dV \quad \text{and} \quad S_{eff}=\int_S\left(\frac{\sigma_e(x,y,z)}{\sigma^*}\right)^m dS \qquad (3)\ (4)$$

In the equations above $\sigma_e(x, y, z)$ is the equivalent stress at the co-ordinates (x, y, z) used to calculate the effective volume or surface, σ^* is a suitable scaling stress (e.g. the maximum tensile stress or the maximum equivalent stress) and m is again the Weibull modulus. The integration is performed over the whole volume or surface of the test specimen.

This calculation is performed within the FE module by calculating the effective volume and surface of each element and the summing them up.

For the evaluation a suitable equivalent stress model has to be chosen. Different equivalent stress models are discussed in the literature, e.g. the maximum principle stress model, the v. Mieses equivalent stress or the principle of independent action (PIA). The first two mentioned equivalent stress models are widely known. The first principle stress model only counts

the maximum tensile stress in the specimen, the v. Mieses model assumes both tensile and compressive stresses with the same importance.

The equivalent stress according the PIA approach, $\sigma_{e,PIA}$, on the other hand takes only the non-negative (i.e. tensile) principle stresses σ_I, σ_{II} and σ_{III} into account. It is assumed that the different tensile stress components act independently and that their net effect according the probabilities of failure is expressed as a weighted accumulation (5),

$$\sigma_{e,PIA} = \sqrt[m]{\sigma_I^m + \sigma_{II}^m + \sigma_{III}^m}\,, \tag{5}$$

with m being the Weibull modulus.

Based on these different equivalent stress models V_{eff} and S_{eff} of the specimens (no. 1) can be calculated and the gained strength values can be converted to a specimen (no. 2) with different V_{eff} or S_{eff} according to [11]:

$$\sigma_e(2) = \sigma_e(1) \cdot \left(\frac{V_{eff}(1)}{V_{eff}(2)} \right)^{1/m}. \tag{6}$$

Experiments on Al_2O_3 specimens

For the experimental verification of the FE investigations tests were performed on Al_2O_3 discs. The material was a standard AL23 (supplied by Friatec) with a diameter of 20 mm and a thickness of 3 mm. The discs were both tested with the as sintered surface as well as with a machined (a grinding finish with diamond grit D15 on the prospective tensile surface) surface. Furthermore small bending samples were machined out of these discs to perform 4-point bending tests as a comparative uniaxial test. For all test conditions 30 samples were tested to allow a meaningful Weibull analysis of this tests. The results of these tests are summarised in table 2. In this table the two Weibull parameters, the characteristic strength, σ_0, and the Weibull modulus, m, are listed as well as its 95% confidence intervals. The strength values listed are the first principle stress values and the PIA equivalent stress values.

From this table it can be seen that the results of the strength tests (σ_0, m) differ quite significantly when only the maximum principle stresses are compared. A obvious result is that the samples with the machined surface have the higher strength values. Two different effects are claimed for

causing the observed effect: Machined the surface reduces the size of flaws and therefore the measured strength is higher. Additionally compressive residual stresses in the tensile surface might be induced during the machining. For the evaluation this residual stresses were assumed to be 0.

TABLE 2: Results of the strength tests on Al_2O_3 specimens.
Listed is the characteristic strength σ_0 (i.e. the maximum tensile stress in the bars or disc), and the Weibull modulus, m, both with a 95% confidence interval in brackets. Furthermore the uniaxial tensile stress results based on the PIA equivalent stress model are shown.

	Test method	σ_0 [MPa]	m	$\sigma_{e,PIA}$ [MPa]	$\sigma_{e,PIA}^{V_{eff}}$ [MPa]	$\sigma_{e,PIA}^{S_{eff}}$ [MPa]
"as sintered" surface	4-point bending	338 (330 / 346)	15 (11 / 18)	338 (330 / 346)	338 (330 / 346)	338 (330 / 346)
	ball on three balls	348 (343 / 354)	17 (14 / 21)	363 (358 / 370)	357 (352 / 363)	334 (329 / 340)
machined surface	4- point bending	365 (359 / 371)	21 (16 / 26)	365 (359 / 371)	365 (359 / 371)	365 (359 / 371)
	ball on three balls	385 (380 / 390)	21 (16 / 26)	398 (393 / 403)	386 (381 / 391)	371 (366 / 376)

The second result is that for the same surface conditions the ball on three balls test shows significantly higher strength values compared to the bending test results. To compare the strength values correctly identical effective volumes or surfaces have to be taken into account. In this work the results of the ball on three balls test are converted to the effective volume and surface of the 4-point bending test. Even for this case using the maximum principle stress model the strength results still differ significantly. The same holds for the v. Mieses equivalent stress approach. Finally the results of the PIA equivalent stress model are also shown in table 2 considering the effective volume $\sigma_{e,PIA}^{V_{eff}}$ and surface $\sigma_{e,PIA}^{S_{eff}}$. It was found that the confidence intervals of the different test methods overlap if the strength values are recalculated to the same effective surface using the PIA approach.

The next logical step is to investigate if these tests are indeed surface sensitive. If this is the case then the fracture has to start at or very near the surface of the discs and bending bars. To prove this the fracture surfaces of the discs and bars were investigated using a SEM. Figure 3 shows a typical fracture origin near the surface.

All analysed fracture origins were at or at least very near the tensile stress surface of the discs and bending bars. This actually shows that these tests

are indeed surface sensitive, at least for the material investigated.

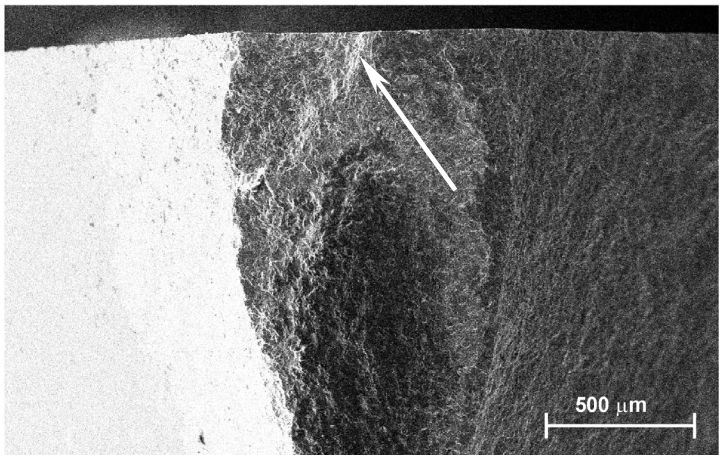

Figure 3: Fracture origin at the surface of a sample tested in the ball on three balls test. The origin is indicated with an arrow.

REFERENCES

1. de With, G., Wagemans, H.M. (1989), *J. Am. Ceram. Soc.*, **72**, 1538
2. Morrell, R., McCormick, N.J., Bevan, J., Lodeiro, M., Margetson, J. (1999), *Brit. Ceram. Trans.* **98**, 234
3. Fessler, H., Fricker, D.C. (1984), *J. Am. Ceram. Soc.* **67**, 582; correction: 1988,**71**,(10), 904
4. Matthewson, M.J., Field, J.E. (1980), *J. Phys. Eng.*, Sci. Instrum., **13**, 355
5. Godfrey, D.J., John, S. (1986), *Proceedings 2nd Internat. Conference of Ceramic materials and Components for Engines*, Verlag Deutsche Keramische Gesellschaft, Lübeck-Travemünde, 14.-17. April 657
6. Börger, A., Supancic, P., Danzer, R. (2001), *J. Eur. Ceram. Soc.,* in Press
7. Shetty, D.K., Rosenfield, A.R., McGuire, P., Bansal, G.K., Duckworth, W.H. (1980), *Ceramic Bulletin*, **59**, 1193
8. Kirstein, A.F., Woolley, R.M. (1967), *J. Res. Natl. Bur. Stand.*, Sect. C, **71**, 1
9. Danzer, R. (1992), *J. Eur. Ceram. Soc,* **10***, 461*
10. Danzer, R., Lube, T., Supancic, P. *(2001) Zeitschrift f. Metallkunde,* **92**, 773
11. Munz, D., Fett, T. (1999) Ceramics, Springer (Ed.), Berlin Heidelberg, Germany